

Dielectric function of nanocrystalline silicon with few nanometers (<3 nm) grain size

Maria Losurdo, Maria Michela Giangregorio, Pio Capezzuto, Giovanni Bruno, M. F. Cerqueira, E. Alves, and M. Stepikhova

Citation: *Appl. Phys. Lett.* **82**, 2993 (2003);

View online: <https://doi.org/10.1063/1.1569052>

View Table of Contents: <http://aip.scitation.org/toc/apl/82/18>

Published by the [American Institute of Physics](#)

Articles you may be interested in

[Ellipsometric study of silicon nanocrystal optical constants](#)

Journal of Applied Physics **93**, 4173 (2003); 10.1063/1.1538344

[Simple model for the dielectric constant of nanoscale silicon particle](#)

Journal of Applied Physics **82**, 1327 (1998); 10.1063/1.365762

[Influence of nanocrystal size on optical properties of Si nanocrystals embedded in SiO₂ synthesized by Si ion implantation](#)

Journal of Applied Physics **101**, 103525 (2007); 10.1063/1.2730560

[Optical functions of chemical vapor deposited thin-film silicon determined by spectroscopic ellipsometry](#)

Applied Physics Letters **62**, 3348 (1998); 10.1063/1.109067

[Complete microcrystalline p-i-n solar cell—Crystalline or amorphous cell behavior?](#)

Applied Physics Letters **65**, 860 (1998); 10.1063/1.112183

[Optical and photoconductive properties of discharge-produced amorphous silicon](#)

Journal of Applied Physics **48**, 5227 (2008); 10.1063/1.323553



Scilight

Sharp, quick summaries illuminating
the latest physics research

Sign up for FREE!

AIP
Publishing

Dielectric function of nanocrystalline silicon with few nanometers (<3 nm) grain size

Maria Losurdo,^{a)} Maria Michela Giangregorio, Pio Capezzuto, and Giovanni Bruno
Institute of Inorganic Methodologies and of Plasmas IMIP-CNR, via Orabona, 4-70126 Bari, Italy

M. F. Cerqueira and E. Alves

Departamento de Física, Universidade do Minho, Campus de Gualtar 4710-057 Braga, Portugal

M. Stepikhova

Institute for Physics of Microstructures, Russian Academy of Sciences, 603600 Nizhny Novgorod GSP-105, Russia

(Received 2 January 2003; accepted 21 February 2003)

The dielectric function of nanocrystalline silicon (nc-Si) with crystallite size in the range of 1 to 3 nm has been determined by spectroscopic ellipsometry in the range of 1.5 to 5.5 eV. A Tauc-Lorentz parameterization is used to model the nc-Si optical properties. The nc-Si dielectric function can be used to analyze nondestructively nc-Si thin films where nanocrystallites cannot be detected by x-ray diffraction and Raman spectroscopy. © 2003 American Institute of Physics.

[DOI: 10.1063/1.1569052]

During the last few years, nanocrystalline silicon (nc-Si) films have received great attention in photovoltaics¹ and optoelectronics.^{2,3} Visible photoluminescence (PL) in the range from 770 to 880 nm, depending on crystallite size, has been reported⁴ for nc-Si with a grain size in the range from 1 to 3 nm due to a quantum confinement effect, overcoming the impossibility of crystalline silicon (c-Si) to emit light because of its indirect band gap. Nanocrystals of silicon have been demonstrated recently to act as sensitizer for erbium ions (Er³⁺) incorporated in a silicon-based matrix,⁵ and to be the most efficient method for obtaining luminescence at 1.54 μm . These applications have in common silicon nanocrystallites with a diameter lower than 3 nm. Optimization of devices requires thin-film nanostructure optimization, understanding of the correlation between the nanostructure and optical/electrical properties and, hence, detection of silicon nanocrystallites volume fraction and size distribution.

Conventional structural diagnostics, such as Raman spectroscopy and x-ray diffraction (XRD) cannot detect nanocrystallites with a grain size lower than 50 Å.⁶ High-resolution transmission electron microscopy (HRTEM) allows direct detection of very small nanocrystals, but it is destructive and not applicable as a routine analysis.

In this letter, spectroscopic ellipsometry (SE) is demonstrated to be useful for nondestructive detection of silicon nanocrystals with a grain size well below 3 nm and for determination of their volume fraction. The dielectric function of nc-Si with a size distribution in the range from 1 to 3 nm is determined. This is an extension to the nanometer scale of the live interest in parameterization and determination of dielectric function of microcrystalline silicon,^{7,8} whose dielectric function is crystallite-size dependent.

Undoped and Er-doped nc-Si films were deposited by reactive rf magnetron sputtering in a reactive atmosphere

($R = p_{\text{H}_2} / (p_{\text{H}_2} + p_{\text{Ar}}) = 0.67$; p = pressure) on ordinary glass substrates at room temperature.⁹ Rutherford backscattering (RBS) was used to determine the atomic composition that resulted in % Si = 72%, % H = 28%, % O < 0.5% (Er doping level $\sim 0.1\%$). HRTEM measurements were performed to establish the presence of silicon nanocrystallites. SE measurements of the pseudodielectric function, $\langle \epsilon \rangle = \langle \epsilon_1 \rangle + i \langle \epsilon_2 \rangle$, were performed in the range from 1.5 to 5.0 eV with a phase-modulated spectroscopic ellipsometer (UVISEL-Jobin Yvon).

SE spectra were analyzed in terms of optical models based on the Bruggeman effective medium approximation (BEMA);¹⁰ the fit goodness was estimated by the parameter χ^2 defined in Ref. 11. A simple two-layer (four-phase) model (substrate/film/SiO₂/air) was used in the analysis. The presence of the native oxide layer was confirmed by x-ray photoelectron spectroscopy while a very low surface roughness (rms = 2 Å) was measured by atomic force microscopy. Standard dielectric functions of a nonhydrogenated amorphous silicon (a-Si),¹² hydrogenated amorphous silicon (deposited in our reactor by plasma-enhanced chemical vapor deposition (PECVD) from a SiH₄-H₂ plasma) were tested in the BEMA modeling. The nc-Si phase was parameterized by the Tauc-Lorentz (TL) expression.¹³ In spite of some limitations of the TL expression recently discussed in Ref. 14. Here it is used with reliable results, as evidenced by the fact that a very simple BEMA model was necessary to fit data with very low χ^2 value and low values (≤ 0.3) of the correlation matrix coefficients for fit parameters. The reliability of the ellipsometric analysis is also corroborated by the good agreement with TEM data.

Figure 1 shows a cross-sectional HRTEM image of a typical nc-Si sample. The micrograph shows that the a-Si:H matrix contains a high density of small clusters that, on the basis of the electron diffraction analysis, have been identified as silicon nanocrystals. The (111) planes of silicon nanocrystals are visible in Fig. 1. The statistical analysis of the nanocrystallites size distribution indicates a mean radius of 1.5 nm.

^{a)} Author to whom correspondence should be addressed; electronic mail: cscpm118@area.ba.cnr.it

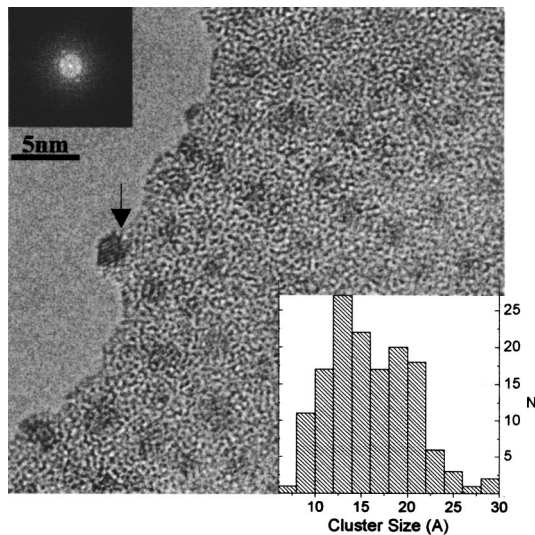


FIG. 1. Cross-sectional TEM image of a nc-Si film deposited on Corning glass. The arrow points out the (111) oriented nanocrystallite. Si nanocrystallite size distribution is also shown.

The silicon nanocrystals are homogeneously distributed within the film thickness that was estimated to be 1400 nm from cross-sectional TEM. This data supports the use of a simple two-layer model in the ellipsometric analysis.

Figure 2 contrasts the SE spectra of the imaginary ($\langle \epsilon_2 \rangle$) part of the pseudodielectric function of a fully amorphous a-Si:H film with $[H]=34\%$, as estimated by RBS, and of the nc-Si:H sample with $[H]=28\%$, whose TEM picture is in Fig. 1. Both $\langle \epsilon_2 \rangle$ spectra are characterized by the peak at about 3.6 eV characteristic of a-Si:H, however, they differ in the interference fringes system, as shown by the inset. In particular, despite the larger hydrogen content that is known to increase the optical band gap, the interference system stops at about 1.9 eV for the a-Si:H film, while it extends up to 2.4 eV for the nc-Si:H sample that has a lower hydrogen content. This indicates an optical band gap for the nc-Si:H sample larger than that of the a-Si:H sample that cannot be ascribed to hydrogen; rather, the band gap increase is due to a quantum confinement effect for nc-Si film, and hence gives

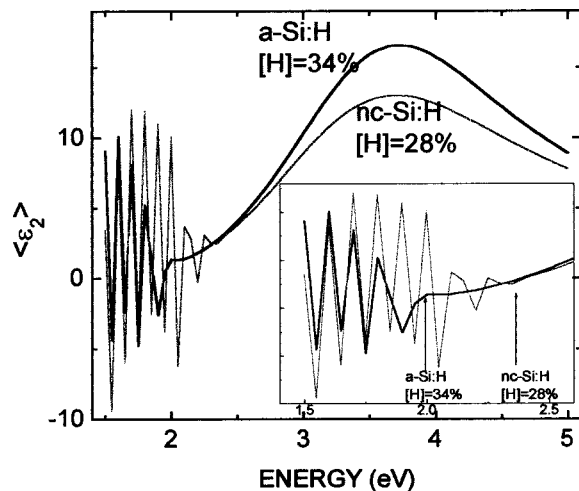


FIG. 2. Experimental SE spectra of the imaginary part ($\langle \epsilon_2 \rangle$) of the pseudodielectric function of a-Si:H with $\%H=34\%$ and of a nc-Si film with $\%H=28\%$. The inset shows the detail of the extend of the interference system.

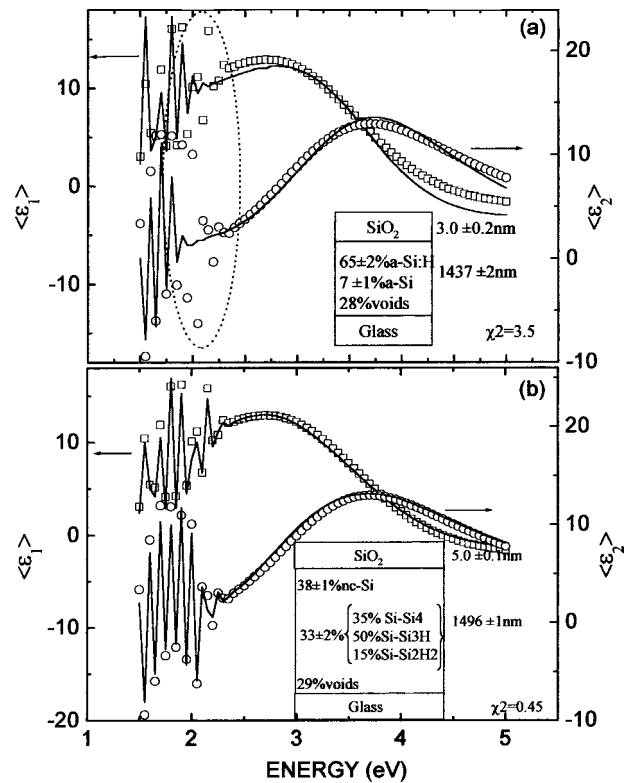


FIG. 3. Experimental (circles) and calculated SE spectra of the real ($\langle \epsilon_1 \rangle$) and imaginary ($\langle \epsilon_2 \rangle$) parts of the pseudodielectric function of a nc-Si film on Corning glass; (a) and (b) show, respectively, the calculated spectra considering the matrix as amorphous-only and with nanocrystallites. The corresponding best-fit BEMA models and fit quality χ^2 are also reported.

SE qualitative evidence of the presence of nanocrystallites.

Figure 3 shows the measured and fitted SE spectra of the same nc-Si sample of Fig. 1. In particular, Fig. 3(a) shows that a poor fit ($\chi^2=3.5$) to the measured pseudodielectric function is obtained by a BEMA model, including an amorphous component a-Si¹² or a-Si:H produced by PECVD and voids, especially in the region of interference fringes. Consequently, it is reasonable (from the TEM data) to assume the film consisting of an a-Si:H phase with inclusion of silicon nanocrystallites. A TL equation parameterizes the nc-Si component. The amorphous tissue has been described, on the basis of the overall hydrogen content ($[H] \sim 28\%$) and of the tetrahedron model¹⁵ as a mixture of Si-Si₄, Si-Si₃H and Si-Si₂H₂ tetrahedra, with relative amounts of 35%, 50%, and 15%, respectively.¹⁶ Figure 3(b) shows the improvement in the fit obtained by the BEMA model including nc-Si and sketched in the inset. The void volume fraction takes into account grain boundaries, and introduces some disorder in the amorphous matrix. Furthermore, hydrogen bond distribution of the amorphous tissue is also consistent with Fourier transform infrared spectrum that showed the peak at 2000 cm^{-1} due to monohydride Si-H stretching with a small shoulder at 2100 cm^{-1} due to dihydride Si-H₂.

The imaginary part of the dielectric function derived for the nc-Si is shown in Fig. 4, together with the corresponding TL parameters. Here, the comparison with the dielectric functions of both a-Si (from CVD) and a-Si:H (from PECVD) is also shown. A small variation of the TL parameters and, hence, of the amplitude and peak position of the dielectric function has been observed depending on the nc-Si

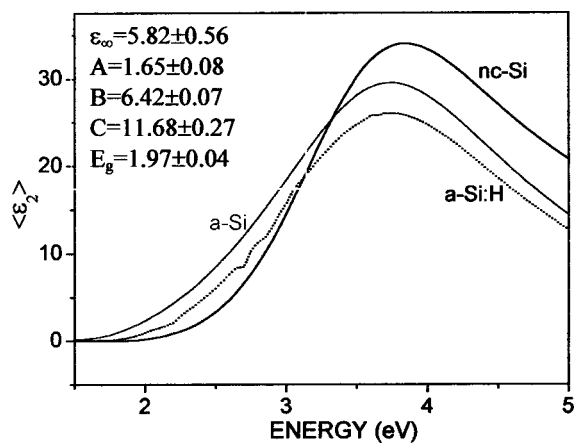


FIG. 4. Calculated SE spectrum of the imaginary part ($\langle\epsilon_2\rangle$) of the dielectric function of nc-Si with an average crystallite size of 1.5 nm. The comparison with a-Si from Ref. 11, and a-Si:H from PECVD is shown as are parameters of TL equation.

size distribution. The main features of the nc-Si dielectric function are the zero absorption up to 2 eV. A band-gap energy of 1.97 ± 0.04 eV has been determined by the TL parameterization. Calculations, by the pseudopotential calculations of Refs. 17 and 18 and by the linear combination of atomic orbital calculations of Ref. 19, predict this band-gap energy value for nanocrystallites of silicon with a size lower than 2 nm. The peak at about 3.8 eV for nc-Si is also consistent with the fact that the dielectric function of the nanosized crystallites should have a very large broadening of the E_1 and E_2 interband critical points characteristic of c-Si and μ c-Si until they merge in a unique peak centered at 3.8 eV.

This approach can be used by other workers to analyze amorphous/nanocrystalline mixed-phase films. In fact, the different hydrogen content can be taken into account by different volume fractions (that are fit parameters) of the $\text{Si}-\text{Si}_{4-v}\text{H}_v$ tetrahedral that describe the amorphous phase; any damage (caused by plasma or grain boundaries effect) is taken into account by the fit variable voids volume fraction. Furthermore, the parameterized equation derived in this work can be used as “a starting point” to determine the dielectric function of a nanocrystalline phase with a different grain size distribution and/or impurity content.

The determined dielectric function of nc-Si can now be used in BEMA analysis of nc-Si samples to find correlation between nanostructure and functional property. An example of this analysis is shown in Fig. 5. Here, IR PL spectra of nc-Si films doped with Er are shown. The samples have the same Er concentration of 0.1% and about the same hydrogen content of $\text{H}\% \sim 27\% - 28\%$ (as determined by RBS). The corresponding XRD and Raman spectra indicated them as amorphous, but on this basis their different PL properties could not be explained. In contrast, the SE analysis indicates that samples differ in the volume fraction of the nanocrystallites, and the larger the volume fraction of nanocrystallites, the higher the PL efficiency at $1.54 \mu\text{m}$ of Er^{3+} ions, because of the efficient transfer of energy from nanocrystals to Er^{3+} as reported by others.⁴

In conclusion, the dielectric function of nc-Si with a crystallite size distribution in the range of 1 to 3 nm has been

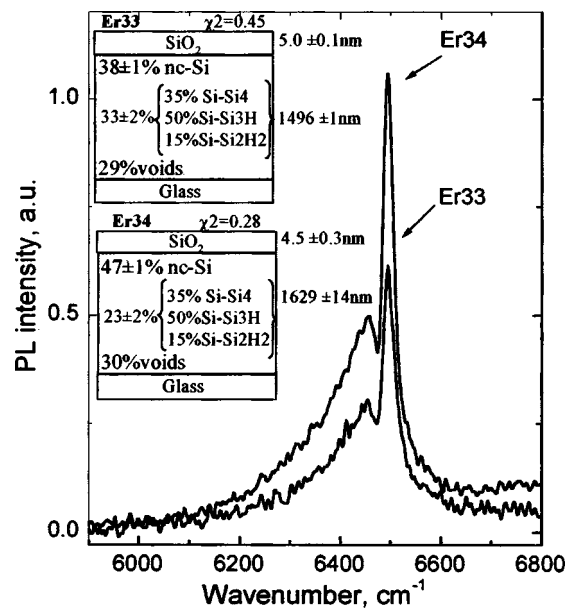


FIG. 5. PL spectra of nc-Si:H ($\text{H}\% = 27\% - 28\%$) with different nc-Si densities and doped with Er ($\text{Er}\% = 0.1\%$).

determined by spectroscopic ellipsometry. The analysis of SE spectra of nc-Si samples is based on a parameterization of the nc-Si dielectric function with the Tauc–Lorentz equation and on a BEMA description of the amorphous phase using the tetrahedron model. It has been shown that spectroscopic ellipsometry can be used to study nondestructively the nanostructure of nc-Si thin films and determine quantitatively the volume fraction of nanocrystallites.

Authors acknowledge Dr. P. Rocai Cabarrocas (Ecole Polytechnique, Palaiseau, France) for helpful discussion.

- R. J. Koval, C. Chen, G. M. Ferreira, A. S. Ferlauto, J. M. Pearce, P. I. Rovira, C. R. Wronsky, and R. W. Collins, *Mater. Res. Soc. Symp. Proc.* **715**, A6.1.1 (2002).
- A. Fontcuberta i Morral and P. Roca i Cabarrocas, *Thin Solid Films* **383**, 161 (2001).
- P. Roca i Cabarrocas, A. Fontcuberta i Morral, and Y. Poissant, *Thin Solid Films* **403–404**, 39 (2002).
- F. Iacona, G. Franzò, and C. Spinella, *J. Appl. Phys.* **87**, 1295 (2000).
- G. Franzò, D. Pacifici, V. Vinciguerra, F. Priolo, and F. Iacona, *Appl. Phys. Lett.* **76**, 2167 (2000).
- A. H. Mahan, J. Yang, S. Guha, and D. L. Williamson, *Phys. Rev. B* **61**, 1677 (2002).
- T. D. Kang, H. Lee, S. J. Park, J. Jang, and S. Lee, *J. Appl. Phys.* **92**, 2467 (2002).
- H. Tourir and P. Roca i Cabarrocas, *Phys. Rev. B* **65**, 155330 (2002).
- M. F. Cerqueira, *Vacuum* **46**, 1385 (1995).
- D. G. Bruggeman, *Ann. Phys. (Leipzig)* **24**, 636 (1965).
- G. E. Jellison, *Thin Solid Films* **313–314**, 33 (1998).
- D. E. Aspnes, A. A. Studia, and E. Kimmsbron, *Phys. Rev. B* **29**, 768 (1984).
- G. E. Jellison and F. A. Modine, *Appl. Phys. Lett.* **69**, 371 (1996); **69**, 2137 (1996).
- A. S. Ferlauto, G. M. Ferreira, J. M. Pearce, C. R. Wronsky, R. W. Collins, X. Deng, and G. Ganguly, *J. Appl. Phys.* **92**, 2424 (2002).
- K. Mui and F. W. Smith, *Phys. Rev. B* **38**, 10623 (1988).
- H. Fujiwara, J. Koh, P. I. Rovira, and R. W. Collins, *Phys. Rev. B* **61**, 10832 (2000).
- L. W. Wang and A. Zunger, *J. Phys. Chem.* **98**, 2158 (1994).
- N. A. Hill and K. B. Whaley, *Phys. Rev. Lett.* **75**, 1130 (1995).
- C. Delerue, G. Allan, and M. Lanoo, *Phys. Rev. B* **48**, 11024 (1993).